ANIR: Atacama Near Infrared Camera for Paschen α Imaging

Kentaro Motohara[a], Natsuko Mitani[a], Shigeyuki Sako[a], Yuka K. Uchimoto[a], Koji Toshikawa[a], Tomoyasu Yamamuro[c], Toshihiro Handa[a], Masuo Tanaka[a], Tsutomu Aoki[b], Mamoru Doi[a], Kimiaki Kawara[a], Kotaro Kohno[a], Takeo Minezaki[a], Takashi Miyata[a], Takao Soyano[b], Toshihiko Tanabe[a], Ken'ichi Tarusawa[b], and Yuzuru Yoshii[a]

[a] Institute of Astronomy, University of Tokyo, Mitaka, Tokyo, Japan;
[b] Kiso Observatory, University of Tokyo, Kiso, Nagano, Japan;
[c] Optcraft, Sagamihara, Tokyo, Japan

ABSTRACT

We have been developing a near infrared camera called ANIR (Atacama Near InfraRed camera), for the University of Tokyo Atacama 1.0m telescope installed at the summit of Co. Chajnantor (5640m altitude) in Northern Chile. The major aim of this camera is to carry out an imaging survey in Paschen α emission line (1.8751μm) from the ground for the first time. The camera is based on a PACE-HAWAII2 array with an Offner relay optics for re-imaging, and field of view is $5.'3 \times 5.'3$ with pixel scale of $0.''308$/pix. It is scheduled to see first light in the end of 2008, and start the Paschen α/β survey of the Galactic plane in 2009.

Keywords: infrared, imager, Paschen alpha, Atacama, Co. Chajnantor

1. INTRODUCTION

To study the formation and the evolution of our Galaxy, it is important to probe distribution of massive star formation activities and ionized gas clouds accompanying to it. However, because most of the star formation activities go on within the Galactic disk, they are hidden by dust extinction and it is difficult to detect them by an optical survey targeted at hydrogen Hα emission line at 0.6563μm.

We therefore focus on hydrogen Paschen α (Paα) emission line at 1.8751μm with the transition of $n = 4$ to 3 . Among the hydrogen recombination lines in the optical to the near infrared wavelength, Paα is one of the strongest. Its intrinsic strength in a typical HII region (Case B, 10000K, $N_{\rm e} = 10^4$ cm^{-3}) is 0.12 of Hα,[1] far much stronger than 0.056 for Paβ at 1.2818μm or 0.0097 for Brγ at 2.1661μm.

In addition, because its wavelength at 1.8751μm is less affected by interstellar dust extinction, Paα is a good indicator for existence of ionizing photons in a dusty environment. Assuming a typical extinction curve[2] and $A_V/E(B-V) = 3.08$, Paα becomes stronger than Hα at $E(B-V) > 1.2$ ($A_V > 3.6$) or than Brγ at $E(B-V) < 28.0$ ($A_V < 86.1$). This means that except at an extremely dense region such as the core of the Galactic center, Paα is the strongest emission line observable. However, it is difficult to carry out its observations from the ground due to the strong atmospheric absorption at 1.8751μm.

The University of Tokyo Atacama 1.0m Telescope[3] is an infrared-optimized telescope located at the summit of Co. Chajnantor (5640m altitude) in Northern Chile. Note that this telescope is also a prototype for the forthcoming 6.5m telescope of the University of Tokyo Atacama Observatory (TAO) project (PI: Yuzuru Yoshii).[4] Thanks to the dry climate and the high altitude, median perceptive water vapor is less than 1mm, and high transmittance in the infrared wavelength is expected. Figure 7 shows the transmittance curve around Paα 1.8751μm. While almost no Paα photon is expected to be detected at a 2600m altitude (this is the height of Paranal, Las Campanas and most of the major observatories in Chile), the transmittance of more than 50% can be expected at Co. Chajnantor.

Atacama Near InfraRed camera (ANIR) is a compact near-infrared imager to carry out not only an ordinary broad-band imaging, but also a Paα emission-line imaging utilizing a narrow-band filter, having been developed

Further author information: (Send correspondence to K.M.) K.M.: E-mail: kmotohara@ioa.s.u-tokyo.ac.jp, Telephone: 81 422 34 5049

Detector	PACE-HAWAII2
Pixel format	1024×1024
Pixel pitch	18.5μm
Readout noise	< 15 e$^-$ r.m.s. (CDS)
Field of view	$5.'25 \times 5.'25$
Pixel scale	$0.''308$/pix
Filter	Y, J, H, K_s, Paα, Paα-off, Paβ

Table 1. Specification of ANIR.

at the Institute of Astronomy, University of Tokyo. It is a simple camera, based on a HAWAII-2 array with an Offner relay optics in it. The overall specification is shown in Table 1.

In Section 2, we describe the overall layout of the instrument. In Section 3, the expected performance will be shown, and in Section 4, we will show preliminary results of the test observations carried out inside Japan.

2. LAYOUT OF THE INSTRUMENT

2.1 Optics

The Offner optics is employed for re-imaging, where the specifications are summarized in Table 2. Both the primary and the secondary mirrors are gold-coated to achieve high reflectivity.

Figure 1 shows spot diagrams of the final image. It can be seen that the spot sizes are smaller than a single pixel throughout the field of view. Figure 2 shows the spot diagrams when a dichroic mirror of fused silica with 7mm thick is insert in front of the dewar window to realize an optical-NIR simultaneous imaging (see Section 2.6 for details), suggesting that the spot sizes are degraded to 3 pixels ($\sim 1''$) at the edge of the field. Therefore, we have also carry out a wave-optics analysis. Figure 3 shows a resulting encircled energy plot of a point spread function at the outer-axis edge of the final image, where the profile is not much degraded from that of a diffraction limited image. Its Strehl ratio in the final image is as good as 0.6, and we conclude that the image degradation by the dichroic mirror is negligible.

2.2 Cryogenics and Mechanics

2.2.1 Cryostat

The cryostat is a compact cube with 260mm on a side (Figure 4, 5). The internal structure consists of three components of a filter box, an Offner optics holder, and a detector box, which is installed on a work surface.

A single stage closed cycle cooler, Cryo-Mini S03Z with cooling capacity of 25W at 77K, manufactured by Iwatani Gas Corp., is adopted. It takes 24 hours to cool down the whole components to a stable temperature. The cold head is detached from the dewar electronically, by inserting insulators at contacts. A sapphire plate with 3mm thick is used as an insulator between the cold head and the heat path, which has high thermal conductivity at cryogenic temperature, and a Teflon plate with 2mm thick between the housing of the cold head and the cryostat.

Effective diameter of primary mirror	90 mm ϕ
Effective diameter of secondary mirror	9 mm ϕ
Curvature radius of primary mirror	140 mm
Offset of optical axis	24 mm

Table 2. Specification of the Offner relay optics.

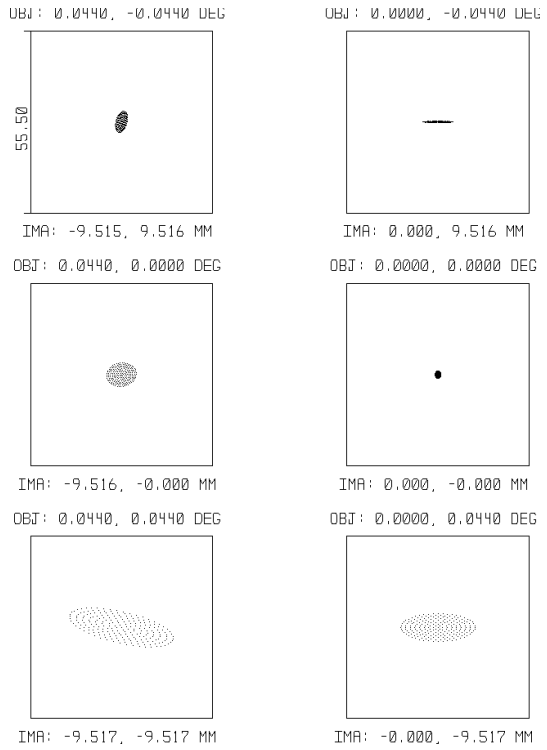

Figure 1. Spot diagrams of the final image. From the upper left to the lower right, each spot corresponds to that at $(2.'6, 2.'6)$, $(0.'0, 2.'6)$, $(2.'6, 0.'0)$, $(0.'0, 0.'0)$, $(2.'6, -2.'6)$, and $(0.'0, -2.'6)$ relative to the center of the image. Squares show boxes with 55.5μm on a side at the focal plane, which corresponds to 3pixels on the detector.

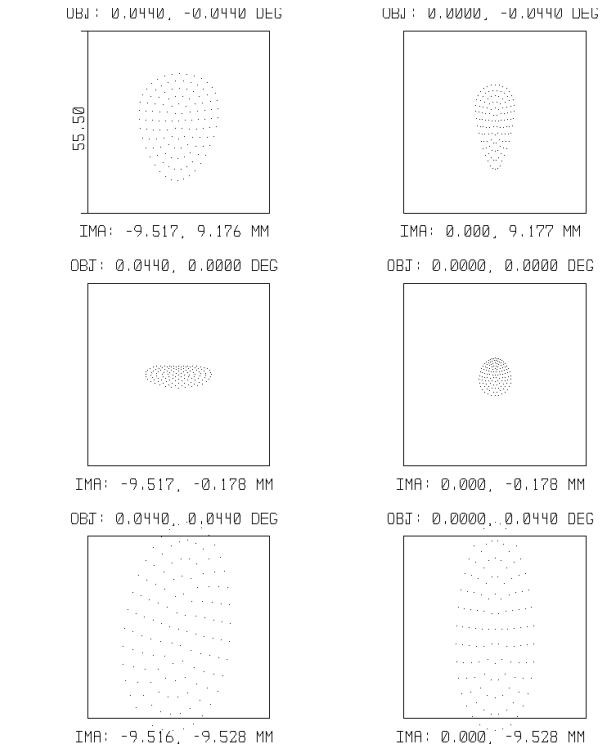

Figure 2. Same as Figure 1, except a dichroic mirror with a wedge angle of 0.78° is inserted in front of the dewar window for a simultaneous optical imaging.

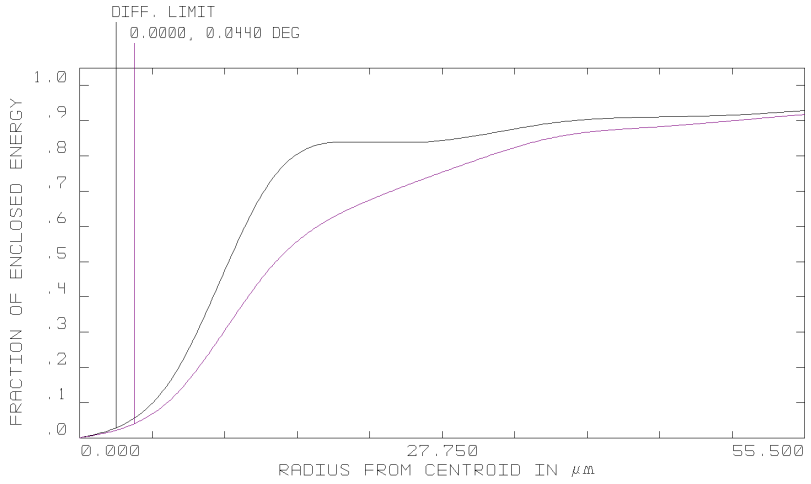

Figure 3. Encircled energy plot at $(0.'0, -2.'6)$ in the final image when the dichroic mirror is inserted in front of the dewar window. The lower magenta line shows an expected profile, while the upper black line shows a profile of a diffraction limited image.

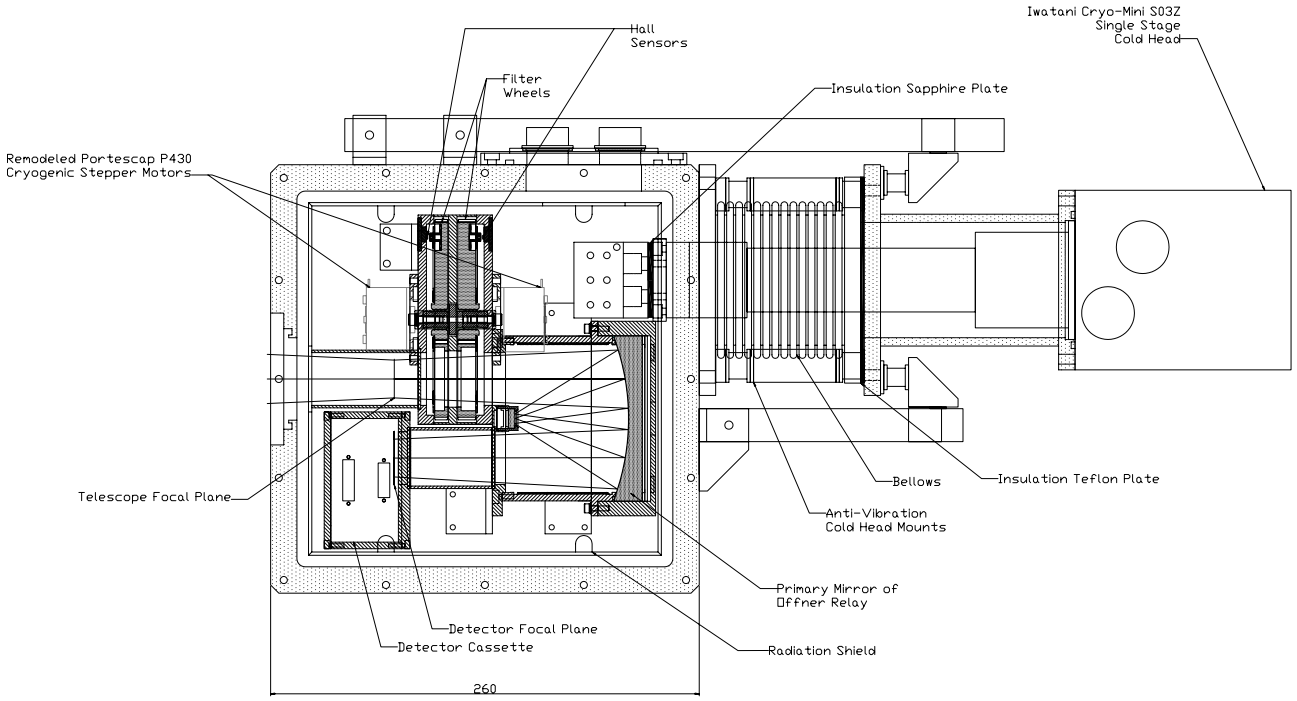

Figure 4. A schematic of the layout inside the cryostat.

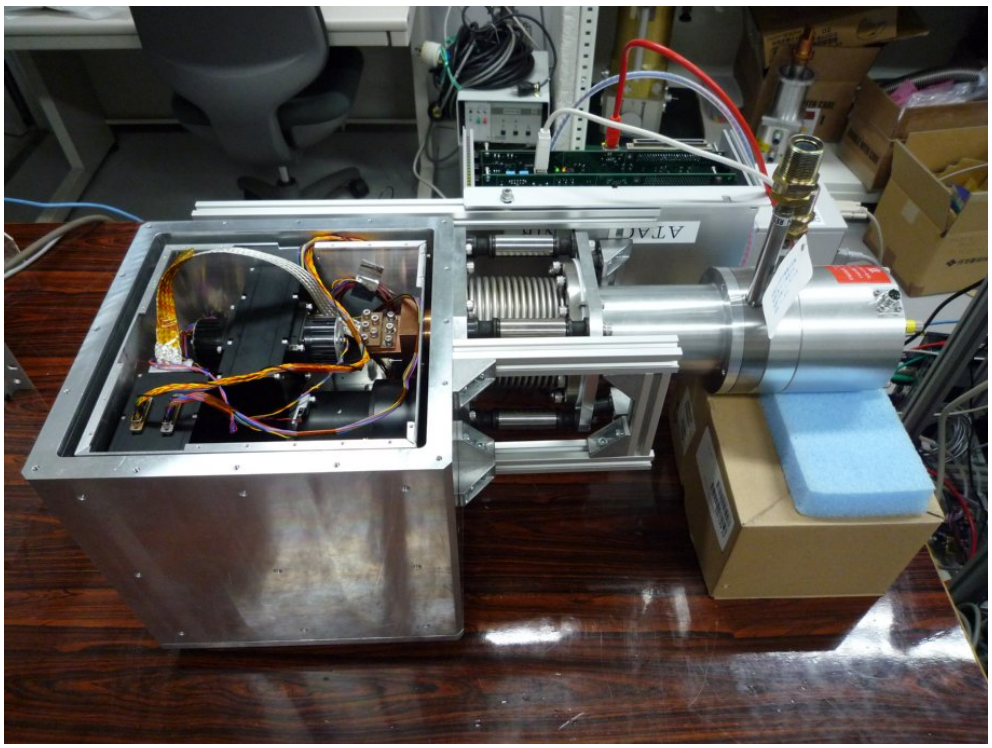

Figure 5. An external view of the cryostat, with all internal components assembled.

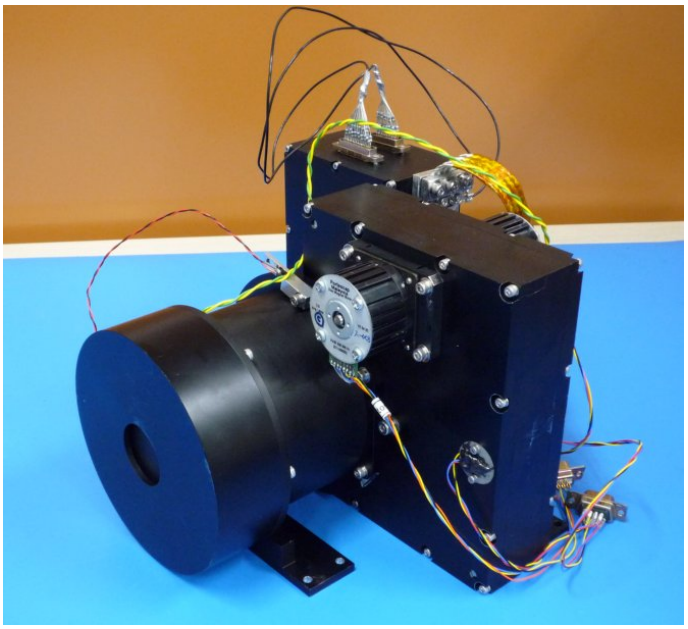

Figure 6. The set-up of the whole internal components, consisting of the Offner optics holder (front left), the filter box (front right), and the detector box (back).

Four thermometers are installed in the cryostat, which are located at the heat sink of the detector, the Offner optics holder, the work surface, and the cold head. These thermometers are driven by a temperature controller Model 330 manufactured by Lake Shore Cryotronics, Inc. It also drives a heater at the detector box to control the detector temperature.

2.2.2 Filter Wheels

Two filter wheels with 5 filter holders each are located just after the telescope focal plane. The first wheel contains four broad-band filters, while the second wheel holds three narrow-bands.

Cryogenic motors based on commercial stepping motors, Portescap P430-258-005 of Danaher Motion Company, are used to rotate these wheels. We have remodeled them by replacing their ball bearings with oil-less bearings MM-SEB95AJ1ZZ1C3/OG of NTN Corp., which incorporate MoS_2 sputtered bearing balls. The motors are driven by a combination of drivers Portescap EDB453-00, and a PCI controller board C-870v1 of Melec Inc. Linux driver software and library for the PCI controller board is newly developed.

Positions of the filter wheels are determined by hall sensors, together with small magnets installed on the wheels. Every filter position has a magnet, and polar character of one magnet in each wheel is reversed to be used as a home position. The hall sensors are driven by an original board, which communicates with the host PC via USB interface.

2.3 Filters

2.3.1 Narrow-Band Filters

Three narrow-band filters for Paα, Paα-off and Paβ imaging are newly designed and fabricated by Optical Coatings Japan whose specifications are summarized in Table 3

Figure 7 shows the atmospheric transmittance and expected background around the Paα wavelength. Due to the complicated transmittance profile around the 1.8751μm, the effective bandwidth of the Paα filter is chosen to be 5nm, which is small enough to cut off the unwanted continuum and still large enough to cover the velocity offset for our scientific observation. The wavelength and the band-width of Paα-off filter is chosen not only for an off-band data-point for the Paα imaging, but also for Paα imaging of extra-galactic objects up to the redshift of $cz = 2600$km/s.

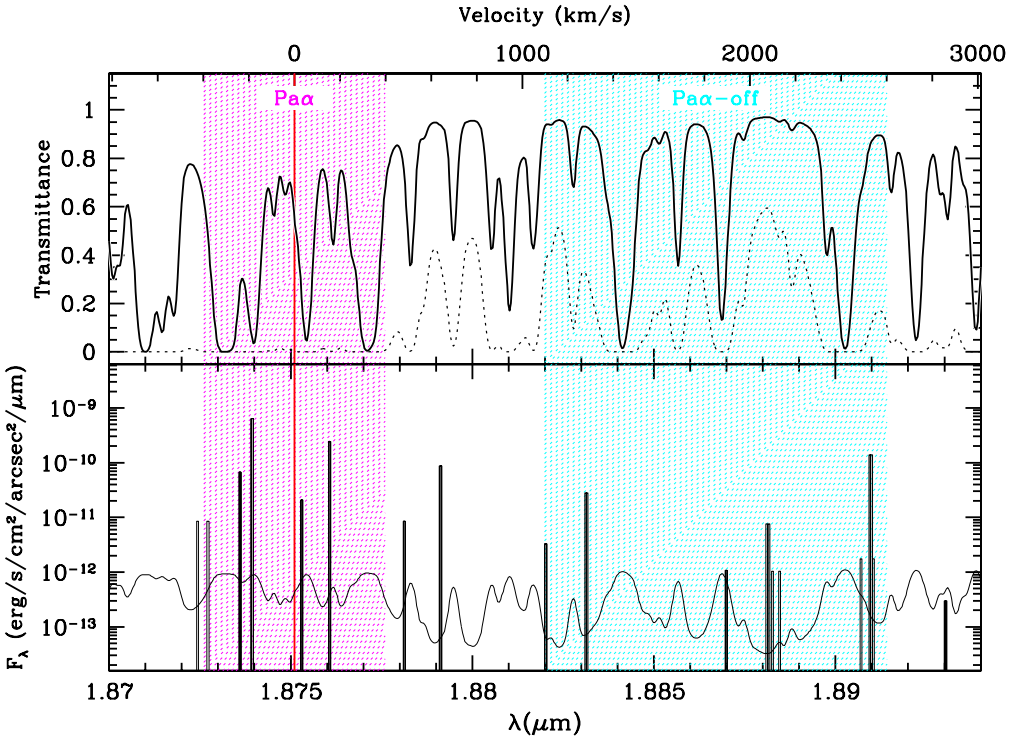

Figure 7. (Top) Atmospheric transmittance at Co. Chajnantor around Paα 1.8751μm, assuming PWV=0.5mm. Dotted line shows that at altitude of 2600m, assuming PWV=6mm. Shaded regions indicate the bandwidths of the narrow-band filters. (Bottom) Expected background. Solid line shows the thermal background from the atmosphere, and spikes show the OH-airglow emission estimated from a laboratory test.

	Paα	Paα-off	Paβ
λ_c (μm)	1.8751	1.8867	1.2818
$\Delta\lambda$ (nm)	< 5	9.4	21
$\lambda_c/\Delta\lambda$	> 375	200	60

Table 3. Specifications of the narrow-band filters.

2.3.2 Broad-Band Filters

Four broad-band filters are also installed for normal imaging, which are the Y, J, H, and K_s of the Mauna Kea observatories near-infrared filter set.[5–7]

2.4 Detector and Array Readout System

2.4.1 Detector

We adopt an engineering-grade PACE HAWAII-2, which is a 2048×2048 HgCdTe near-infrared array manufactured by Teledyne Scientific & Imaging (formerly Rockwell Scientific Company). Of four quadrants of HAWAII-2, only a single quadrant with 1024×1024 pixels is used.

The detector is mounted on a zero insertion force (ZIF) pin grid array socket of 3M Co. Ltd, which is soldered on a fan-out board. The fan-out board is contained in a detector box, and connected to the Offner optics unit (Figure 6). The array is cooled down by connecting a heat sink to pins of the ZIF socket to which unused pins of the ceramic package of the array is inserted. The heat sink is connected to the detector box, and the temperature

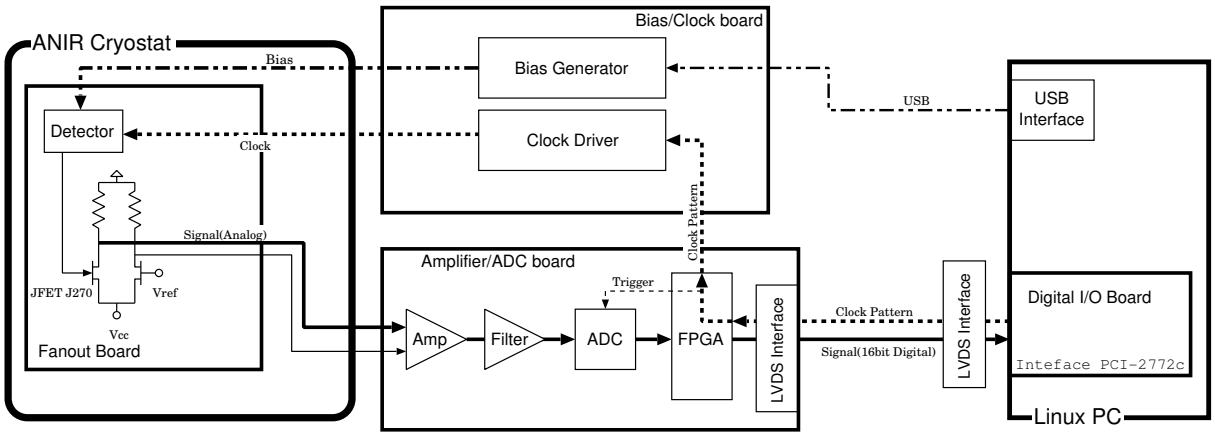

Figure 8. The layout of the readout system of ANIR.

at the heat sink is controlled by the heater attached to the box. In a normal operation, the temperature is set to 77K.

2.4.2 Readout Electronics and Data Acquisition

For the array readout, data acquisition system TAC[8] is adopted, which is originally designed for mid-infrared arrays of MAX-38 camera.[9] The TAC system consist of a real-time Linux PC equipped with a RTAI extension, and a digital I/O board PCI-2772c (Interface Co. Ltd.) with a DMA function. The front-end electronics consist of the fan-out board mentioned above and two VME full-size boards, that is a bias/clock board and an amplifier/ADC board. The overall layout of the readout system is illustrated in Figure 8.

Clock patterns generated at the host PC are first written in a FIFO of the I/O board, and then send to the clock driver on the bias/clock board via amplifier/ADC board. They are then converted to real clocks, and send to the detector. 12 clocks are necessary to drive the detector. 7 biases for the detector are also created on the bias/clock board, whose voltages are controlled from the host PC over USB interface.

Instead of using an on-chip buffer of HAWAII-2 for the signal readout, we choose to install an external buffer to avoid the internal glow of the array.[10] An unbuffered output is send to a source follower on the fan-out board constructed using the JFET J270. This source follower has a identical pair with fixed voltage input, and send to the pre-amplifier on the amplifier/ADC board in differential mode to get rid of external noise input. The signal is then amplified with a gain of 8.4, filtered with a cutoff frequency of 2 MHz and digitized by a 16-bit A/D converter. The digital data is then send to the host PC, and converted to a FITS image. The expected conversion factor is 2.18 e^-/ADU. Pixel rate is set to $3 \sim 8$ μs, corresponding to a readout time of $3 - 8$ s. The measured readout noise of a multiplexer is < 10 e^- with a single correlated double sampling (CDS), small enough for low-background environment achieved by the narrow-band imaging.

2.5 Control System

The block diagram of the whole control system of the instrument is shown in Figure 9. The system is controlled by the host PC with a dual core CPU, running the Linux OS on it with the real-time patch of RTAI. The current system incorporates Intel Core 2 Duo processor with 2 GBytes of memory. Due to the low pressure at the high altitude of 5640m, it is found that the hard disk drives (HDDs) often don't function well. Some of them don't spin up, and some even crash. We therefore use a 32 GBytes SSD (Solid State Disk) based on flash memory, MTRON model SD-S35032GA01. This SSD has fast I/O performance; benchmark testing shows sequential read speed of ∼70 MBytes/sec and write speed of 50–80 MBytes/sec, which are faster than a normal HDD.

The DC power supply for the front-end electronics, the temperature controller, and a vacuum gauge controller is monitored and controlled via RS-232C interface of a terminal server MOXA NPort 5410, which can be operated over TCP/IP network as a normal serial-port device from any PC. The AC 100V power for these units are supplied

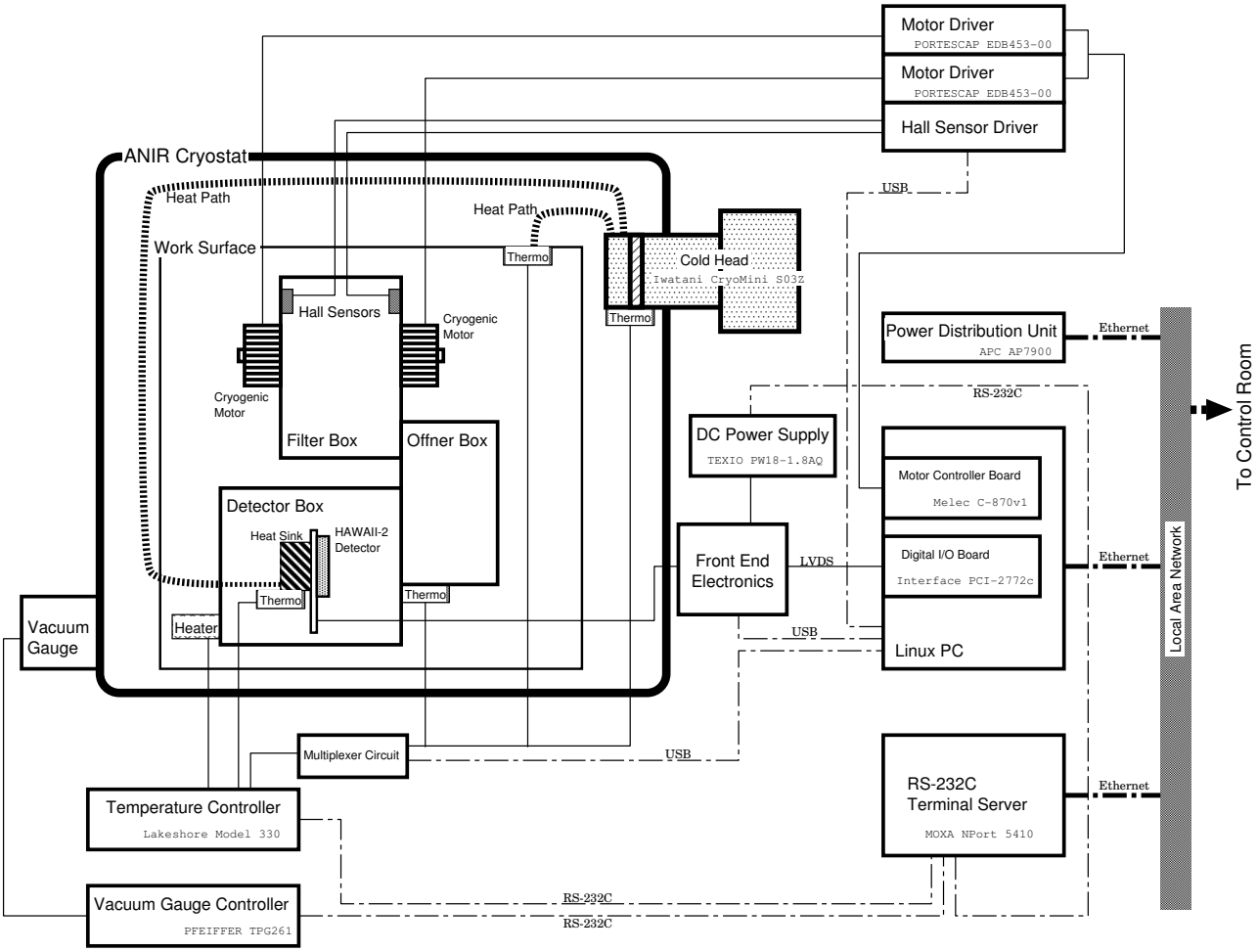

Figure 9. A block diagram of the whole system of ANIR, which is all mounted on the Cassegrain focus of the 1.0m telescope.

from a power distribution unit APC AP7900, of which each outlet is controlled from the control room over the network. They are installed in a rack and mounted on the Cassegrain focus of the 1.0m telescope.

All the status and the house-keeping information are collected by the host PC and registered in a MySQL database server.

2.6 Optical Channel

As an add-on, we are now planning to install an optical camera, which can carry out a simultaneous optical imaging by inserting a dichroic mirror in front of the dewar window of the ANIR cryostat. The size of the dichroic mirror is 50mm $\times$ 71mm, with the substrate thickness of 7mm. The substrate is made of fused silica with a wedge angle of 0.78° to set astigmatism of the final image to the minimum (Figure 2).

The optical light is reflected at the dichroic mirror and re-focused on a CCD after the focal plane is extend by a relay optics. This optical channel is also expected to be used as an auto-guider under low-background observations with the narrow-band filters.

3. EXPECTED PERFORMANCE

The broad-band limiting magnitudes are expected to be $Y = 22.3$, $J = 21.8$, $H = 21.0$, and $K_s = 21.7$ in AB magnitude, with exposure time of 3600s, $S/N = 5$, and aperture diameter of $\phi = 1''$.

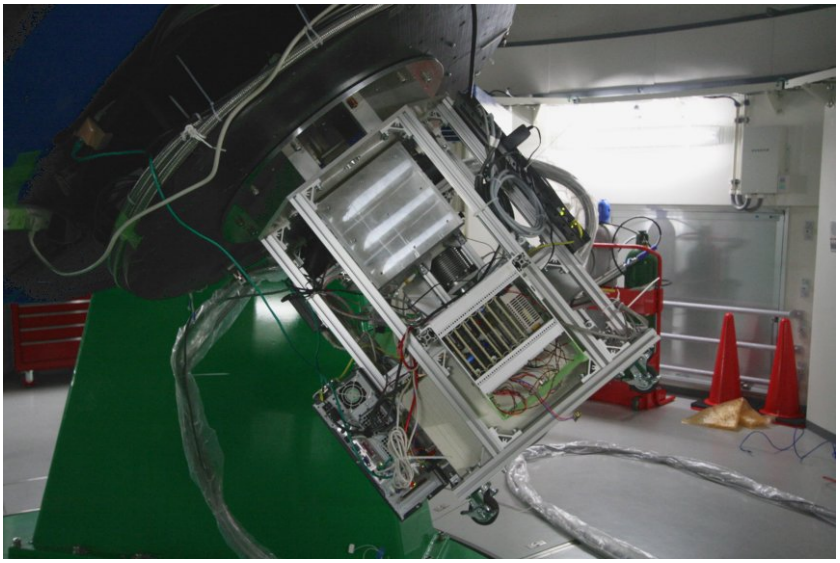

Figure 10. ANIR mounted on the Cassegrain focus of the 1.5m "Kanata" telescope at the Higashi-Hiroshima Observatory.

The limiting magnitude for the Paα narrow-band filter is rather difficult to estimate, especially because there are no measurement of the OH airglow at 1.875μm which falls between the atmospheric windows. We therefore estimate it from the model calculation[11*] whose line strength is scaled by the real measurement at the optical wavelength[12†]. The expected line strength is shown in the lower panel of Figure 7. Limiting flux for the Paα filter is then estimated to be 12 μJy, which corresponds to the emission-line strength of 1×10^{-17} W/m^2/$\square''$ (3600s, $S/N = 5$).

For the optical channel, the limiting magnitudes will become 22–23 AB magnitude (3600s, $S/N = 5$, and $\phi = 1''$) at BVR, although this may vary according to the quantum efficiency of the CCD camera.

4. TEST OBSERVATION

We have carried out a test observation run on Feb. 2008, installing ANIR on the Cassegrain focus of the 1.5m "Kanata" telescope at the Higashi-Hiroshima Observatory operated by the Hiroshima Astrophysical Science Center, Hiroshima University (Figure 10). Because the detector has not been delivered, optical observation using the multiplexer without any filter has been done.

The main purpose is to check

- readout noise,
- performance of the optics,
- internal flexure, and
- total system operability.

There was no major problem found except the readout noise, which couldn't be measured due to an extremely high noise pattern that turned out to be caused by a solder crack on the fan-out board.

*The data is available at http://www.eso.org/sci/facilities/paranal/instruments/isaac/tools/oh/list_v2.0.dat
†The data is available at http://www.eso.org/observing/dfo/quality/UVES/pipeline/sky_spectrum.html

ACKNOWLEDGMENTS

We thank K. Kawabata, M. Uemura, T. Yamashita, T. Ohsugi and the students of the Hiroshima Astrophysical Science Center, Hiroshima University for supporting the test observation at the 1.5m "Kanata" telescope at the Higashi-Hiroshima Observatory. The HAWAII-2 detector has been generously leased by the Subaru Telescope, National Astronomical Observatory of Japan. This work has been supported in part by the Grant-in-Aid for Scientific Research (17104002, 20041003) from Japan Society for the Promotion of Science. S. Sako is financially supported by Japan Society for the Promotion of Science (18-9936). Part of this work has been supported by NAOJ Research Grant for Universities.

REFERENCES

[1] Osterbrock, I. H., [*Astrophysics of Gaseous Nebulae and Active Galactic*], University Science Books, Mill Valley, CA (1989).

[2] Pei, Y. C., "Interstellar dust from the milky way to the magellanic clouds," *ApJ* **395**, 130–139 (1992).

[3] Sako, S., Aoki, T., Doi, M., Handa, T., Kimiaki, K., Kohno, K., Minezaki, T., Mitani, N., Miyata, T., Motohara, K., Soyano, T., Tanabe, T., Tanaka, M., Tarusawa, K., Yoshii, Y., Bronfman, L., and Ruiz, M. T., "The university of tokyo atacama 1.0m telescope," *Proc. SPIE* **7012**, in press (2008).

[4] Yoshii, Y., Doi, M., Handa, T., Kawara, K., Kohno, K., Minezaki, T., Mitsuda, K., Miyata, T., Motohara, K., and Tanaka, M., "Tokyo atacama observatory project," *Proc. of the IAU 8th Asian-Pacific Regional Meeting* **II**, 35–36 (2002).

[5] Simons, D. A. and Tokunaga, A. T., "Mauna kea observatories near-infrared filter set. i. defining optimal $1-5$ micron bandpasses," *PASP* **792**, 169–179 (2002).

[6] Tokunaga, A. T., Simons, D. A., and Vacca, W. D., "Mauna kea observatories near-infrared filter set. ii. specifications for a new $jhkl'm'$ filter set for infrared astronomy," *PASP* **792**, 180–186 (2002).

[7] Tokunaga, A. T. and Simons, D. A., "Mauna kea observatories near-infrared filter set for 1-5 microns," *Proc. SPIE* **4841**, 420–424 (2003).

[8] Sako, S., Miyata, T., Nakamura, T., Motohara, K., Uchimoto, Y. K., Onaka, T., and Kataza, H., "Developing infrared array controller with software real time operating system," *Proc. SPIE* **7021**, in press (2008).

[9] Miyata, T., Sako, S., Nakamura, T., Onaka, T., and Kataza, H., "A new mid-infrared camera for ground-based 30 micron observations: Max38," *Proc. SPIE* **7014**, in press (2008).

[10] Hodapp, K. W., Hora, J. L., Hall, D. N. B., Cowie, L. L., Metzger, M., Irwin, E., Vural, K., Kozlowski, L. J., Cabelli, S. A., Chen, C. Y., Cooper, D. E., Bostrup, G. L., Bailey, R. B., and Kleinhans, W. E., "The hawaii infrared detector arrays: testing and astronomical characterization of prototype and science-grade devices," *New Astronomy* **1**, 177–196 (1996).

[11] Rousselot, P., Lidman, C., Cuby, J. G., Moreels, G., and Monnet, G., "Night-sky spectral atlas of oh emission lines in the near-infrared," *A&A* **354**, 1134–1150 (2000).

[12] Hanuschik, R. W., "A flux-calibrated, high-resolution atlas of optical sky emission from uves," *A&A* **407**, 1157–1164 (2003).